J. Davis

1975

Calspan

BICYCLE TIRE TESTING –
EFFECTS OF INFLATION PRESSURE &
LOW COEFFICIENT SURFACES

Task Order No. 5

J. A. Davis

Calspan Report No. ZN-5431-V-3

Prepared For:

SCHWINN BICYCLE CO.
CHICAGO, ILLINOIS

MAY 1975

Calspan Corporation
Buffalo, New York 14221

FOREWORD

This document completes the reporting under Calspan Contract CC-254 (Internal Work Authorization 652) with the Schwinn Bicycle Company, Chicago, Illinois. The other formal reports, previously issued, are: "The Effects of Frame Properties on Bicycling Efficiency" by J. A. Davis and R. J. Cassidy, Calspan No. ZN-5431-V-2, November 1974, and "Bicycle Dynamics--Simplified Steady-State Response Characteristics and Stability Indices" by R. S. Rice, Calspan No. ZN-5431-V-1, June 1974.

Three additional informal reports resulting from ad hoc tasks have been transmitted to Schwinn: (1) The Influence of Reflectors on Wheel Imbalance (letter of January 31, 1974), (2) Comparison of Bicycle Designs Using Stability Index Values (letter of March 19, 1974), and (3) A Note on Design Criteria for Bicycle Stability in Terms of Front End Geometry (by R. S. Rice, December 1974).

This report has been reviewed and is approved by:

Raymond R. McHenry

Raymond R. McHenry
Assistant Head
Transportation Safety Department

Calspan performed its first bicycle tire testing for Schwinn (Ref. 1) to determine the side force characteristics of a range of bicycle tires as a function of normal load, slip angle, and inclination angle for use in the bicycle computer simulation. The work described in this report extends that data base to include the effects of low inflation pressures and simulated wet road conditions.

The initial set of tire tests was done using a variable geometry fixture on which the bicycle tire and wheel were mounted. This assembly was towed behind a car across an asphalt road surface. Normal load was supplied by a set of weights mounted on the fixture. Extensive corrections were required in the resultant data, since normal load, slip angle, and inclination angle were not purely independent variables. They were mutually dependent to a certain extent and were also affected by the level of side force developed.

To improve the repeatability and accuracy of the test data, it was decided that a new tire test fixture would be built for testing this most recent set of tires. This machine was described in a previous letter to Schwinn (Ref. 2) so no detailed discussion of it will be included here. Briefly, the test tire is mounted in a fixture above a rotating drum ten inches wide and four feet in diameter, which was already available for use at Calspan. A normal load is applied to the tire by a pneumatic cylinder, forcing the tire into contact with the drum. Since the bicycle tire contact patch is small, the drum closely approximates a flat surface. The fixture to which the wheel is mounted is isolated from its supporting structure by a load cell and a ball-bearing-mounted pivot axis parallel to the vertical axis on the tire. All the side force generated by the tire is therefore measured by the load cell. Slip angle is variable from -4 to +10 degrees, and inclination angle from -10 to +45°. To more closely simulate the actual operation of a bicycle tire, both the inclination axis and the slip axis of the fixture pass through the tire contact patch.

Calibrations of the major variables were performed prior to testing. The following are estimates of the accuracy of measurement of these variables during the testing:

Normal Load (F_z)	± 2 lbs.
Side Force (F_y)	± 1 lb.
Slip Angle (α)	$\pm 0.1°$
Inclination Angle (γ)	$\pm 0.5°$

TEST PROCEDURES

Our original test plan called for the testing of four different tires under a total of seven conditions, as described below:

1) Puff Road Racer, 40 psi, dry surface.
2) Puff Road Racer, 20 psi, dry surface.
3) Puff Road Racer, 75 psi, wet surface.
4) Bridgestone Tri-A1, 75 psi, dry surface.
5) Bridgestone Tri-A1, 75 psi, wet surface.
6) HP Sports Touring, 85 psi, wet surface.
7) Straight Side Sports Touring, 60 psi, wet surface.

To this list we added another test condition, a 75 psi test of the Puff Road Racer on a dry surface. This test complements Tests 1, 2 and 3 listed above, but, more importantly, it is a duplicate of a test included in the first set of tire tests, which were run with different test equipment and procedures. Each test condition listed above was run through the ranges of the three major variables shown below:

Normal Force: 50, 100 lbs.
Slip Angle: -2,-1,-1/2,0,1/2,1,2,3,4,6 degrees
Inclination Angle: -10,0,10,20,30,40 degrees

All the tire tests were run at a virtual road speed of 12 mph. The rotating drum has a continuously variable speed control, but has a lower speed limit equivalent to 12 mph.

The surface used for the dry tests was an adhesive-bonded flexible sheet with a coarse granular surface. This material, known as Grade "B" Safety Walk, is manufactured by 3M Corp. and is currently being used for automotive tire tests on Calspan's Tire Research Facility. The coefficient of friction between the Puff Road Racer tire and this surface was 0.94, measured statically with a normal force of 50 lbs. and the lateral force applied at the contact patch parallel to the "y" axis of the wheel.

The simulated wet surface was the bare steel drum coated with a silicone-based lubricant. As long as the surface was kept wet, the coefficient of friction remained very stable. The same test as run on the dry surface gave a coefficient of 0.30 for the simulated wet surface. This compares to a value of 0.30-0.35 for the low coefficient area of our test track.

TEST RESULTS

Figures 1A-8B present the results of the tire tests in terms of side force as a function of slip angle and inclination angle. Data on the previous set of tire tests was presented as a normalized side force function after corrections and a statistical evaluation of the raw data were made. It is believed that the present data were of sufficiently higher quality to enable the presentation of the actual data in the form of carpet plots. This gives considerably more insight into the physical characteristics of the tires, in addition to providing all the necessary data required for the bicycle simulation.

The one correction made in the data was to compensate for the effect of side force on slip angle. The test fixture exhibited 0.1 degree of slip angle compliance for each 13.3 lbs. of side force. This correction was applied to the dry data only, since the average correction required for the wet data was less than 0.1 degree. One point must be clarified before interpreting this corrected data. Since the correction to slip angle was made graphically as a function of side force in Figs. 1-4, the slip angle scale is non-linear. However, this in no way affects the accuracy of the data presented. Also, since there is no correction applied at the origin of each carpet plot, the slopes of the side force vs. slip angle functions at 0° slip (which represent cornering stiffness) are unaffected.

In order to allow a more effective comparison of the data taken at 50 and 100 lb. normal loads, the side force scale factor on the plotted data is proportional to normal load. Also, the side force scale factor for the wet test data is half that of the dry tests, in order to amplify the display of the wet data.

Figure 9 is a plot of the tire data on the Puff Road Racer (75 psi, dry) which was obtained during the first series of tire tests. This test condition can be compared with those of Figs. 1A and B to determine the correlation between the two different test methods. Figure 9, however, is a plot of normalized side force (at 75 lbs. normal load) as a function of slip and inclination angles, while Figures 1A and B are plots of side force vs. slip and inclination angles. Calculating cornering coefficients* gives the following data:

Figure No.	Normal Load	Cornering Coefficient
1A	50	.200
9	75	.167
1B	100	.160

This shows reasonably good correlation between the two methods.

* (The slope of the normalized side force vs. slip angle line at $\alpha = 0°$, $\gamma = 0°$.)

An evaluation of camber coefficients is not as straightforward. In the case of Figure 9, the side force vs. inclination angle function was assumed to be linear, giving a positive camber coefficient at $\gamma = 0°$. In the test of Figs. 1A and B this function is non-linear; in fact, the slope of this function between $\gamma = 0°$ and $\gamma = 10°$ is effectively zero. This is true, or nearly so, for all the tires and conditions tested, leading to the conclusion that, in general, at slip angles around 0° little camber thrust is generated below 10° of camber.

A further review of the data reveals additional significant trends:

- Figs. 1-3, which represent changes in inflation pressure on a single tire, show a noticeable decrease in cornering stiffness with decreasing pressure. No such effect is seen with respect to camber stiffness.

- Normalized side force decreases with increasing normal force, in agreement with the previous tire test results.

- Differences in tire performance can be related to tread design in at least one case. The Bridgestone Tri-Al has two heavy circumferential ribs in the center of the tread, as opposed to the generally smooth, round cross sections of the other high pressure tires. Both the dry and wet data on the Bridgestone Tri-Al show a decrease in camber thrust from 0° camber to a minimum at 20°, and then increasing to a maximum at 40°.

- The data from the simulated wet tests exhibit much lower cornering and camber coefficients than that of the dry tests. Significant differences still exist between tires, however. For example, the Bridgestone Tri-Al achieves almost peak side force at a slip angle of 2°, while the side forces generated by the other tires are still increasing well beyond this point.

REFERENCES

1. Roland, R. D., Jr. and Lynch, J. P.: "Bicycle Dynamics - Tire Characteristics and Rider Modeling", Cornell Aeronautical Laboratory, Inc., Technical Report No. YA-3063-K-2, March 1972.

2. Roland, R. D., and Davis, J. A., "Progress Report - Research in Bicycle Dynamics," May 9, 1974.

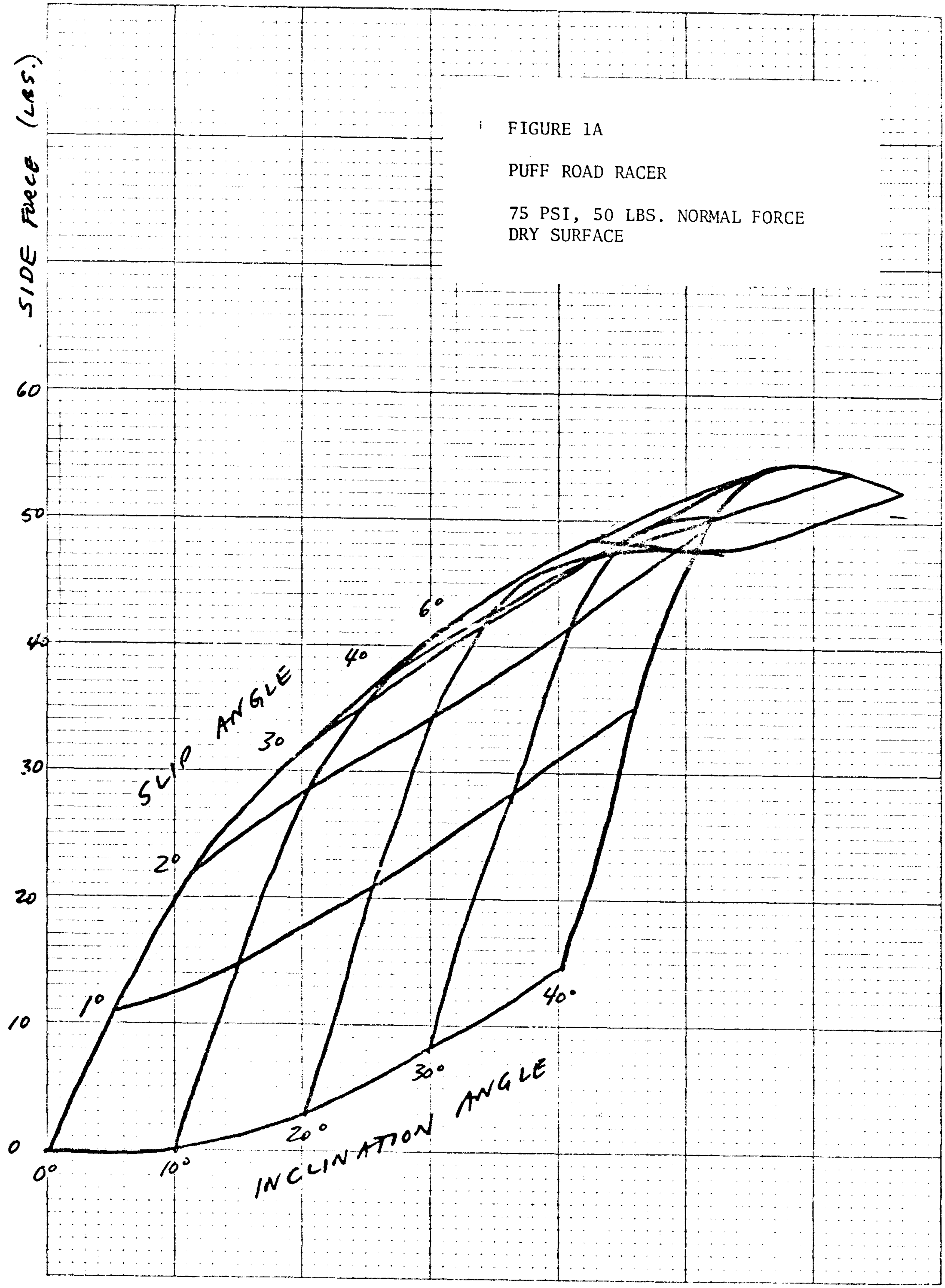

FIGURE 1A

PUFF ROAD RACER

75 PSI, 50 LBS. NORMAL FORCE
DRY SURFACE

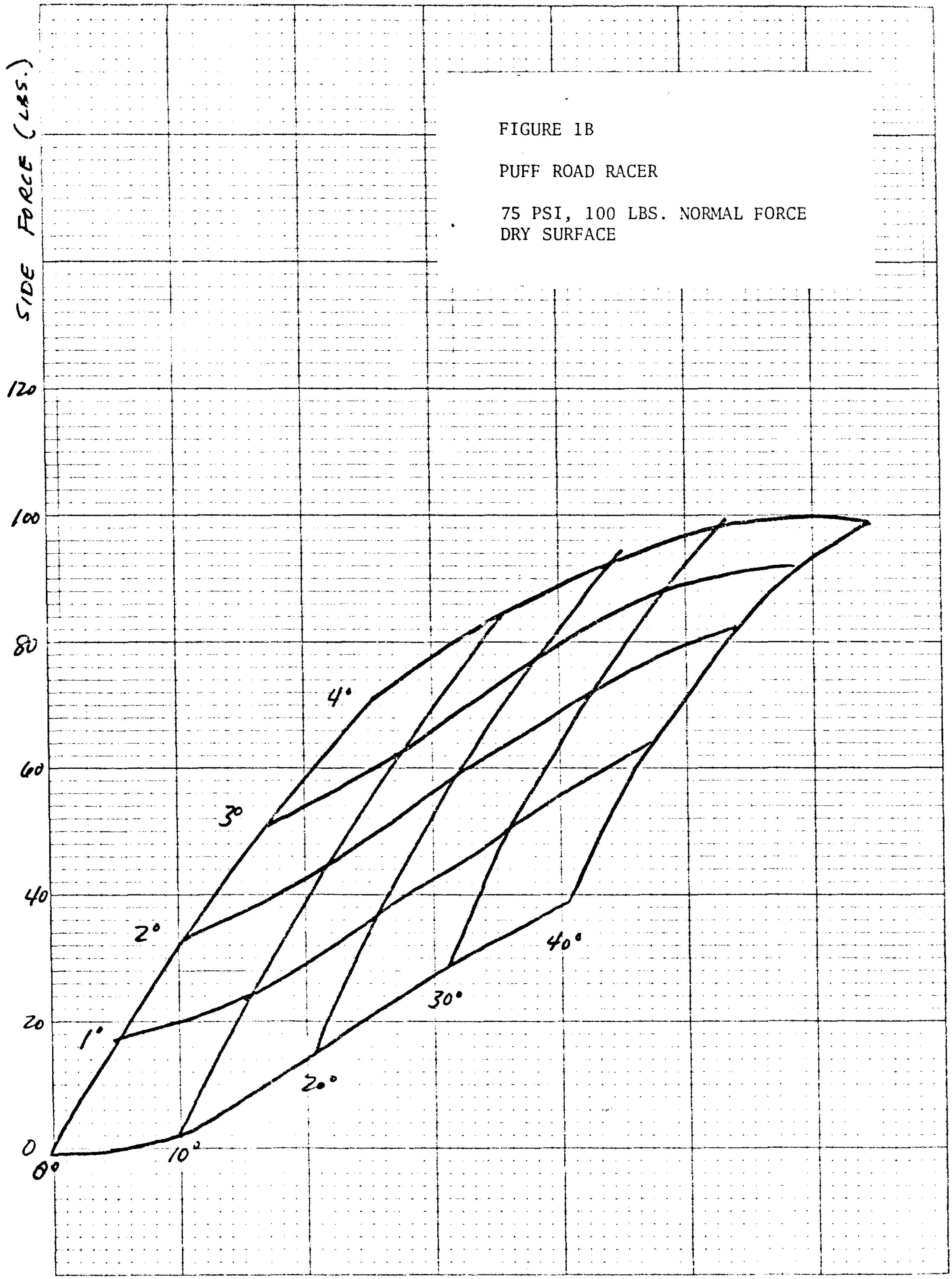

FIGURE 1B

PUFF ROAD RACER

75 PSI, 100 LBS. NORMAL FORCE
DRY SURFACE

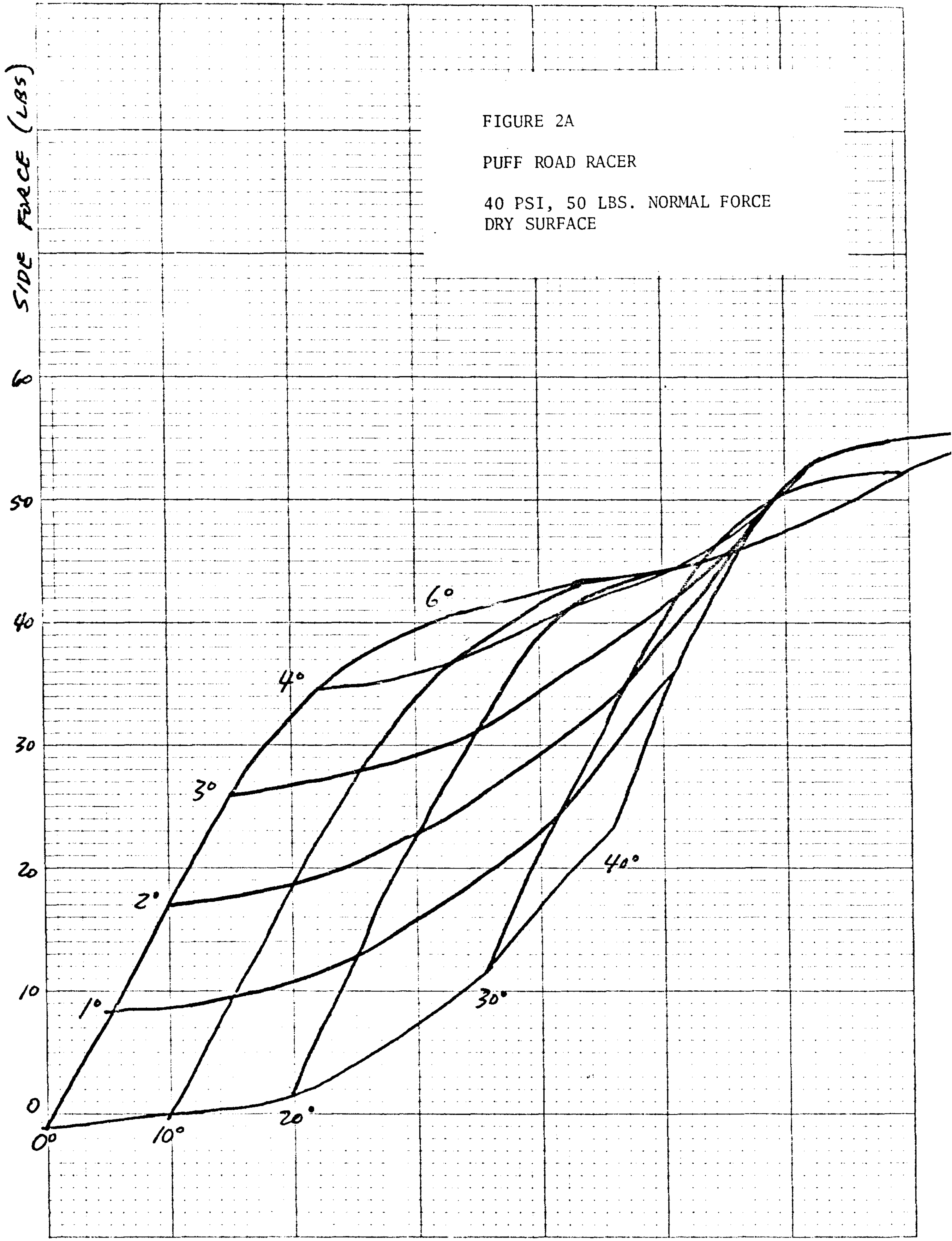

FIGURE 2A

PUFF ROAD RACER

40 PSI, 50 LBS. NORMAL FORCE
DRY SURFACE

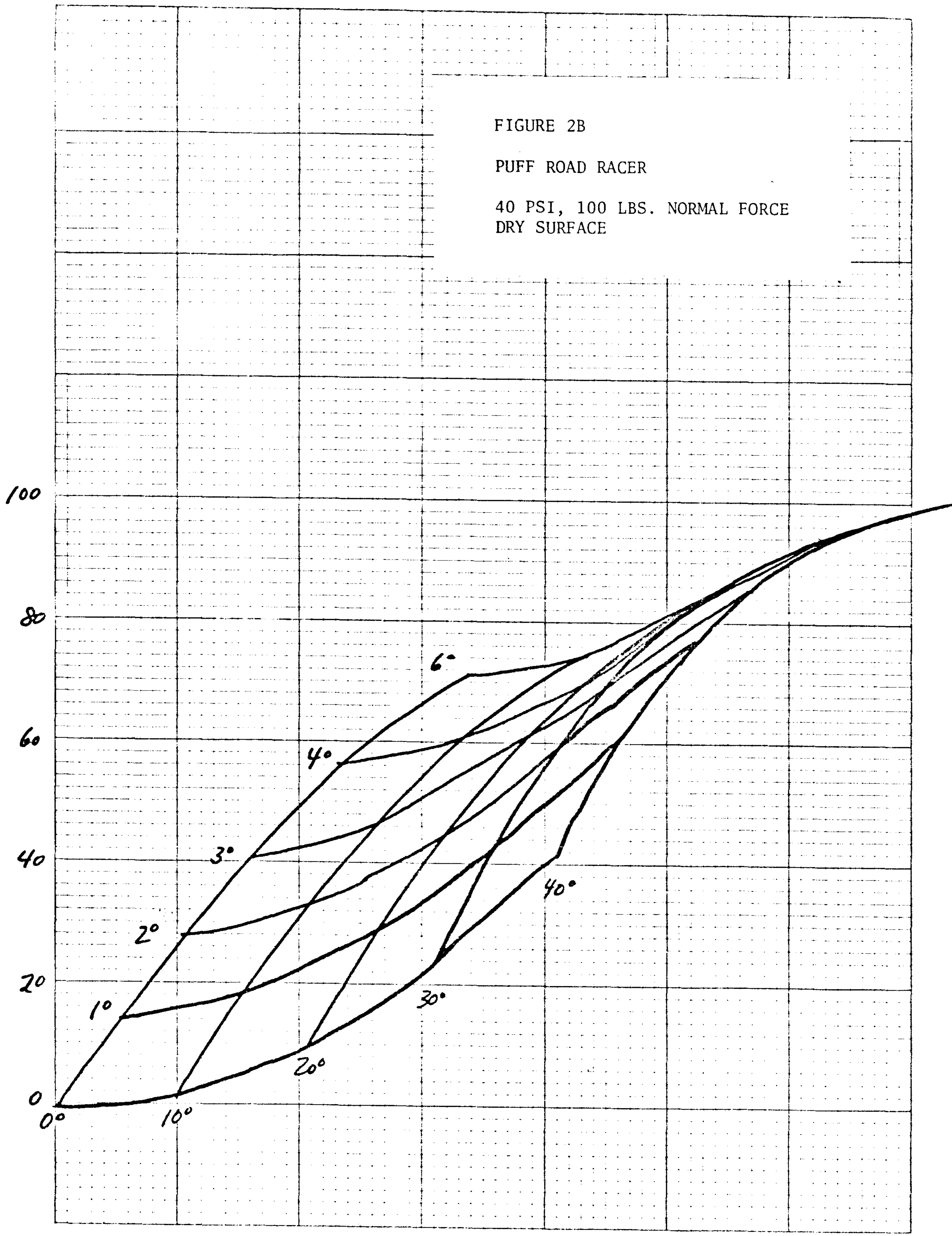
FIGURE 2B
PUFF ROAD RACER
40 PSI, 100 LBS. NORMAL FORCE
DRY SURFACE
100
80
60
40
20
0
0°
10°
20°
30°
40°
1°
2°
3°
4°
6°

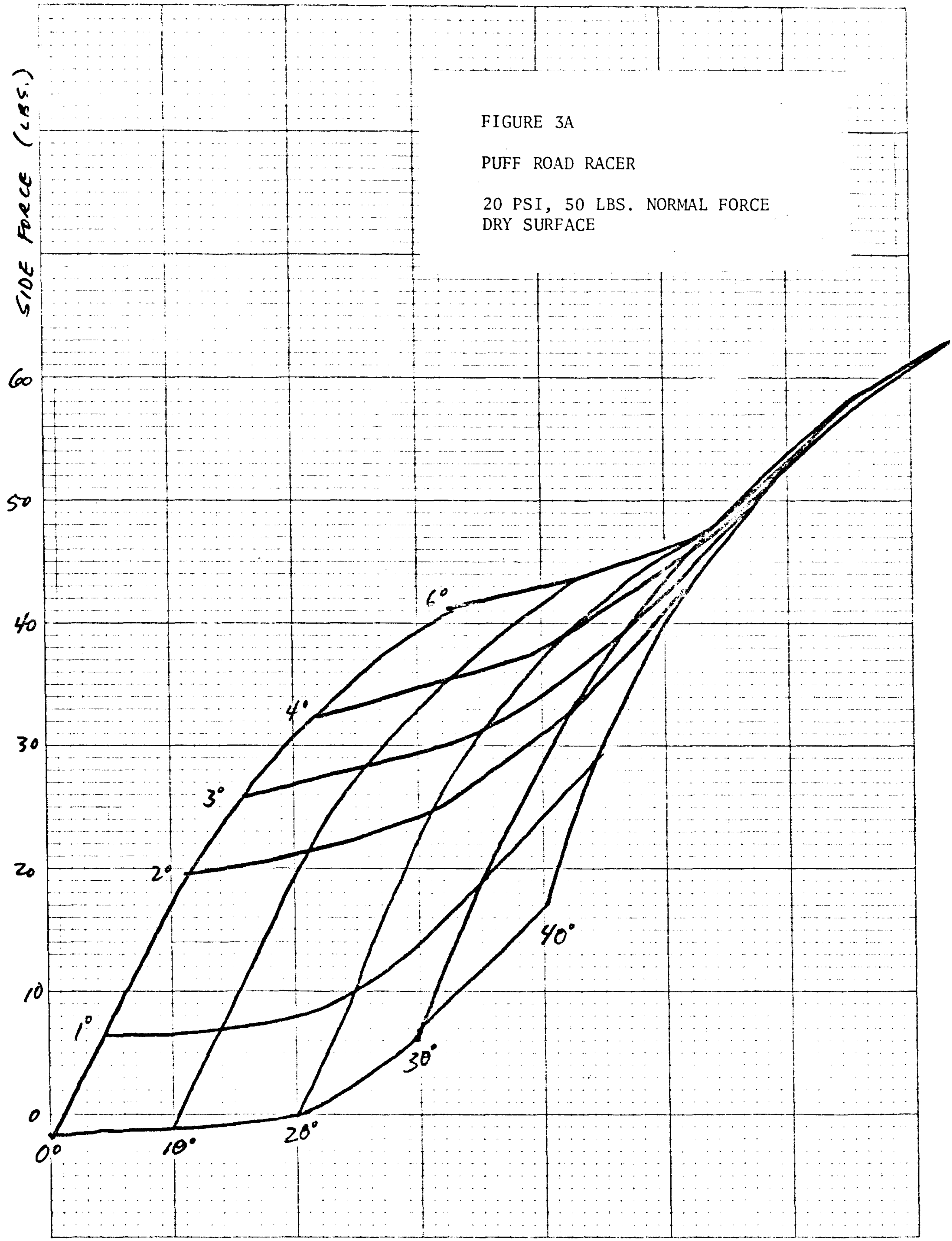

FIGURE 3A

PUFF ROAD RACER

20 PSI, 50 LBS. NORMAL FORCE
DRY SURFACE

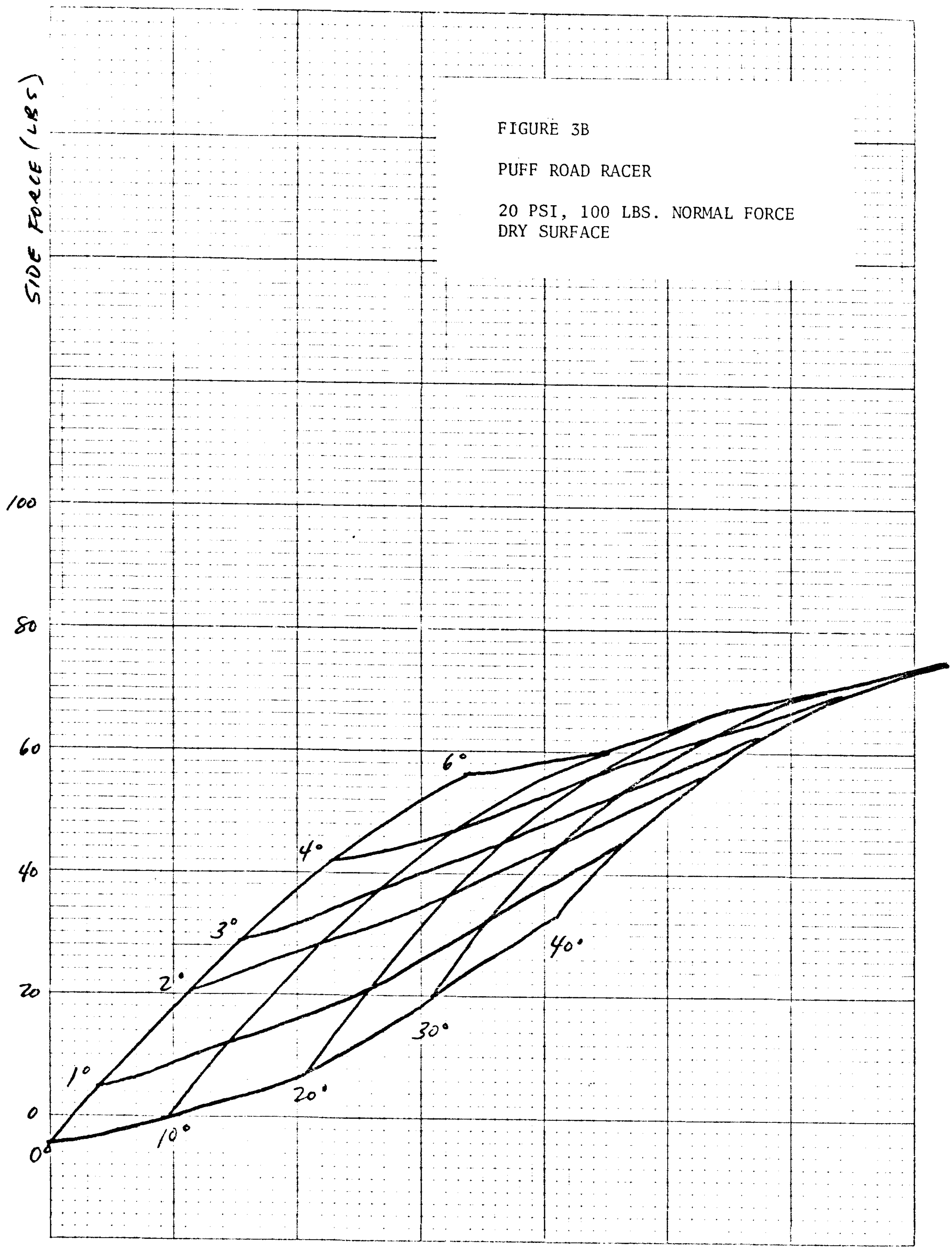

FIGURE 3B

PUFF ROAD RACER

20 PSI, 100 LBS. NORMAL FORCE
DRY SURFACE

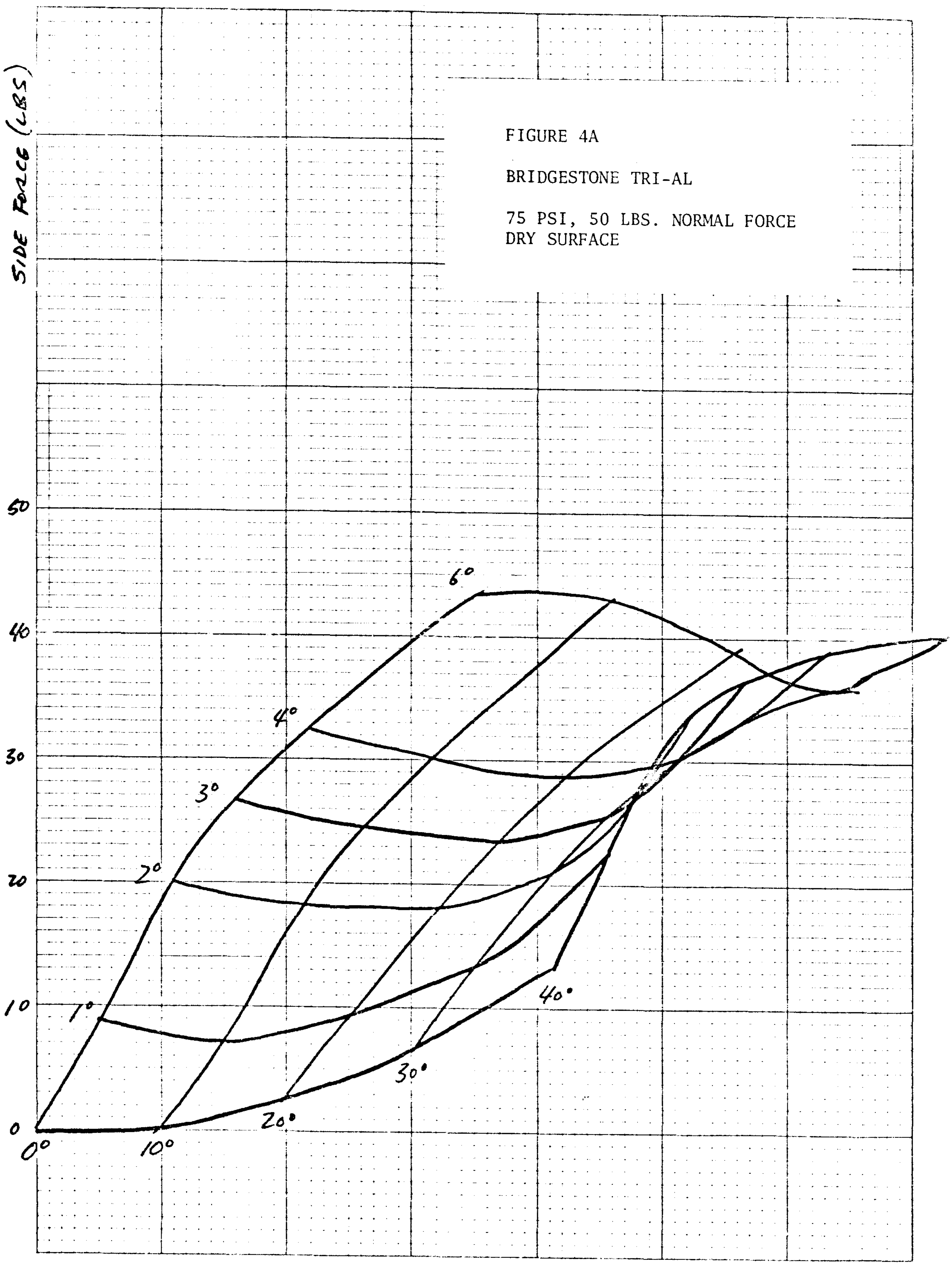

FIGURE 4A

BRIDGESTONE TRI-AL

75 PSI, 50 LBS. NORMAL FORCE
DRY SURFACE

FIGURE 4B

BRIDGESTONE TRI-AL

75 PSI, 100 LBS. NORMAL FORCE
DRY SURFACE

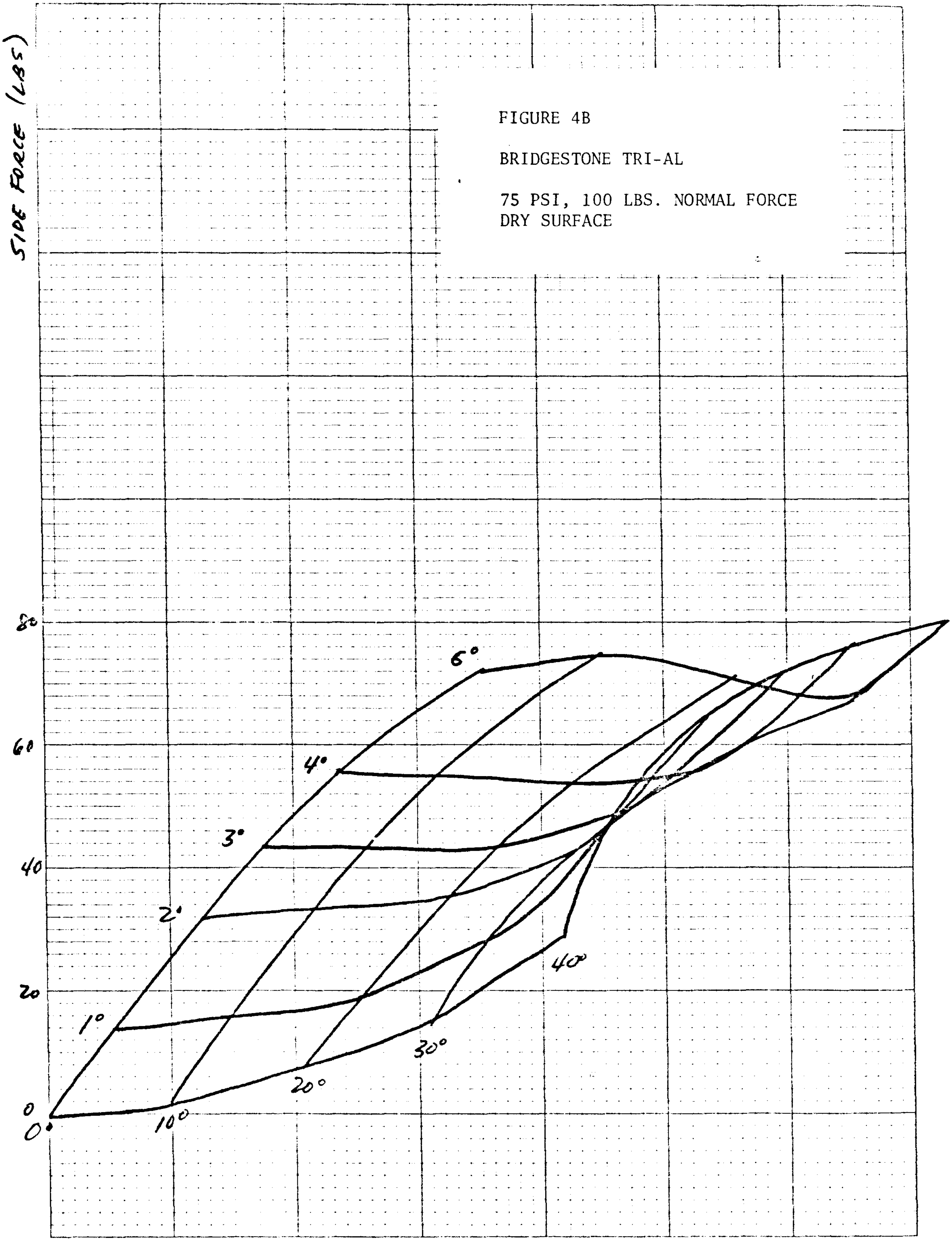

FIGURE 5A

BRIDGESTONE TRI-AL

75 PSI, 50 LBS. NORMAL FORCE
WET SURFACE

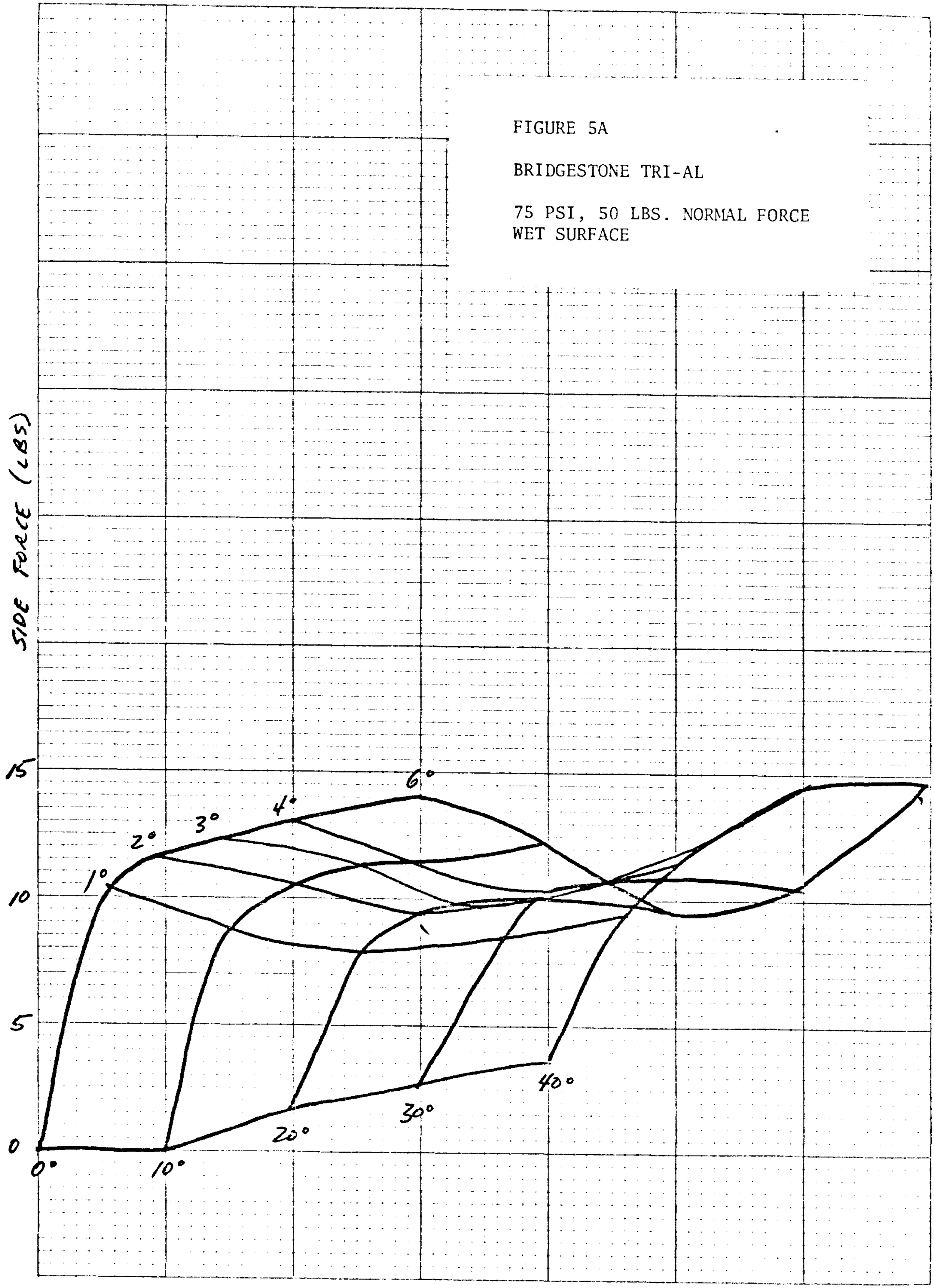

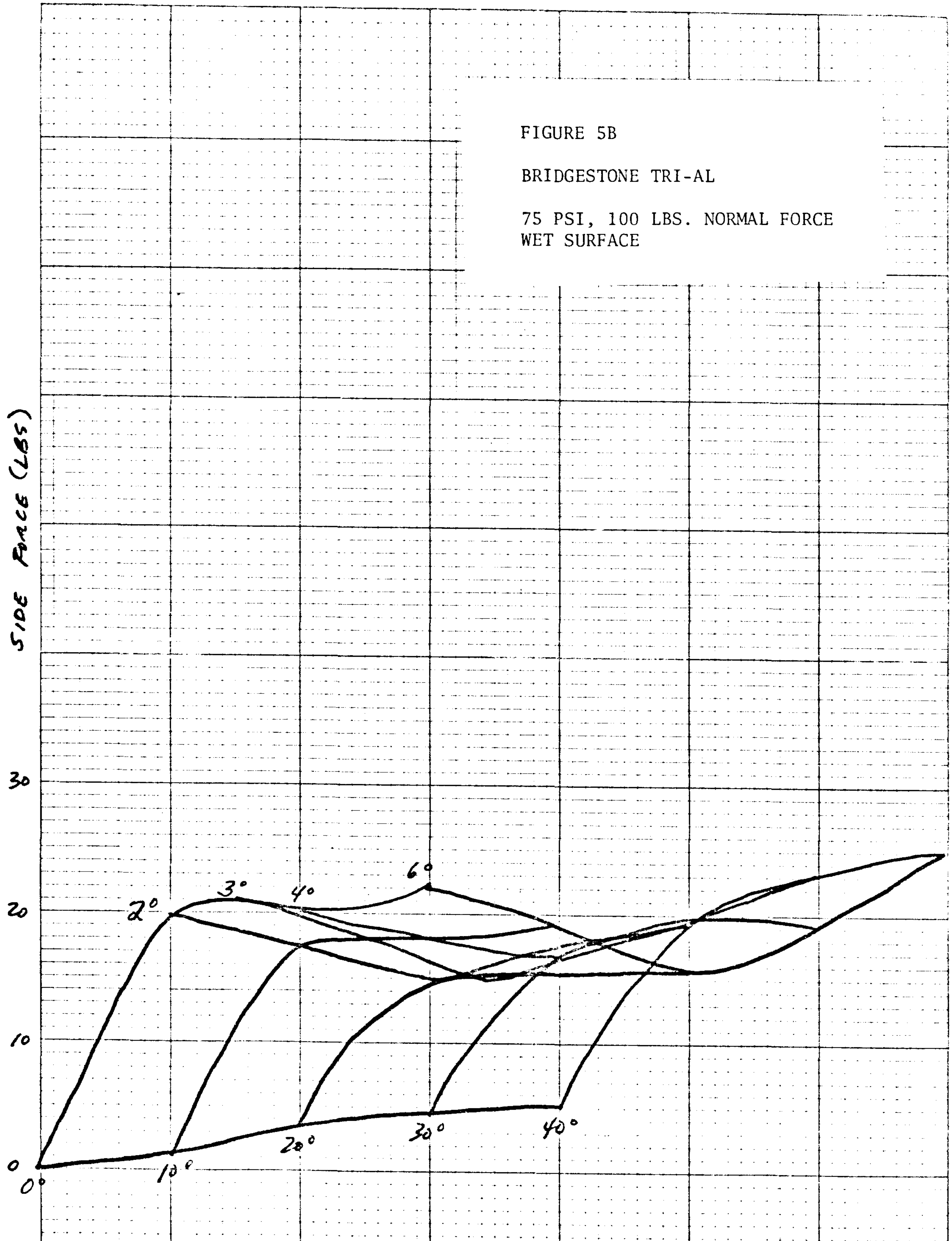

FIGURE 5B

BRIDGESTONE TRI-AL

75 PSI, 100 LBS. NORMAL FORCE
WET SURFACE

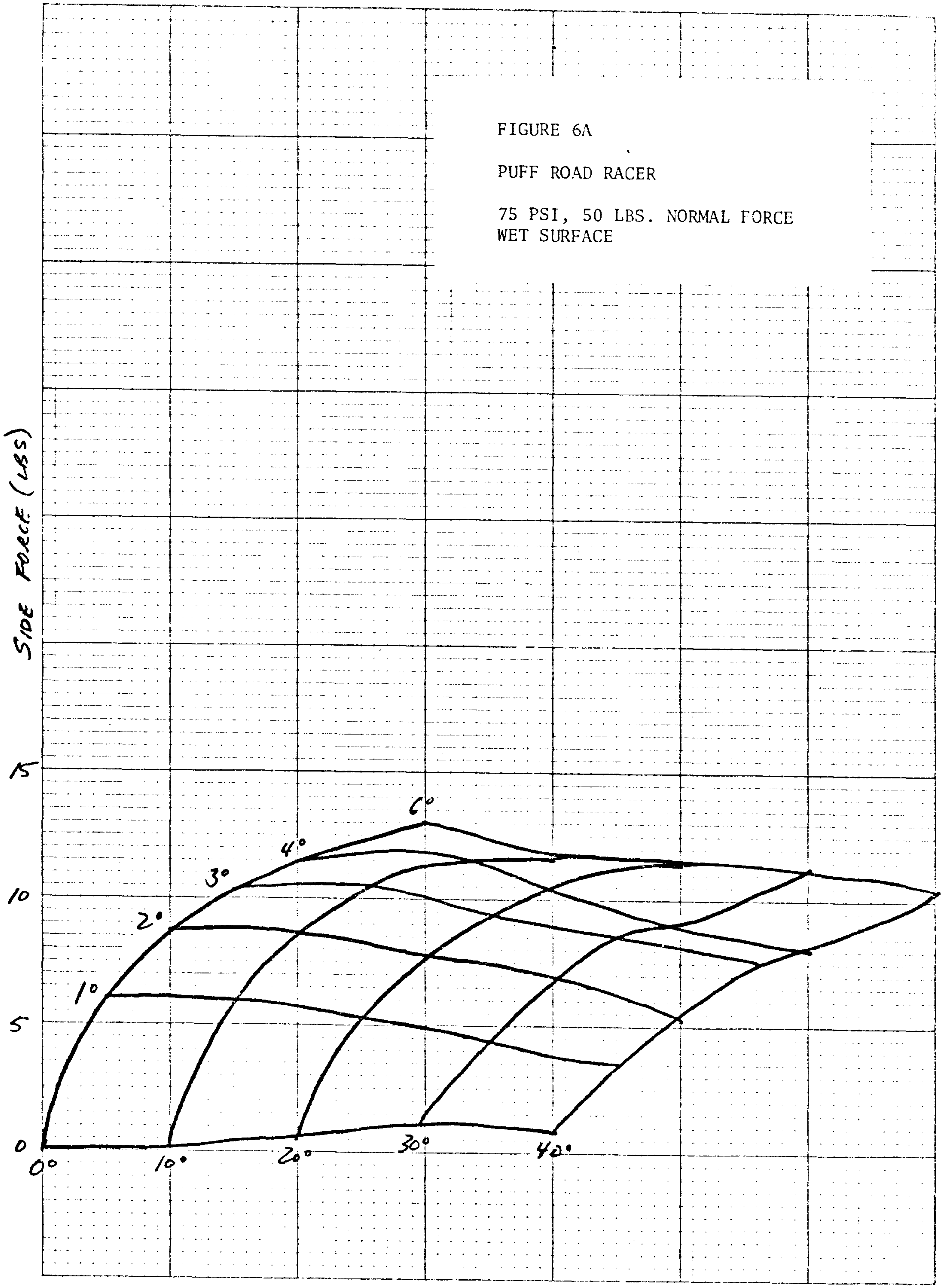

FIGURE 6A

PUFF ROAD RACER

75 PSI, 50 LBS. NORMAL FORCE
WET SURFACE

FIGURE 6B

PUFF ROAD RACER

75 PSI, 100 LBS. NORMAL FORCE
WET SURFACE

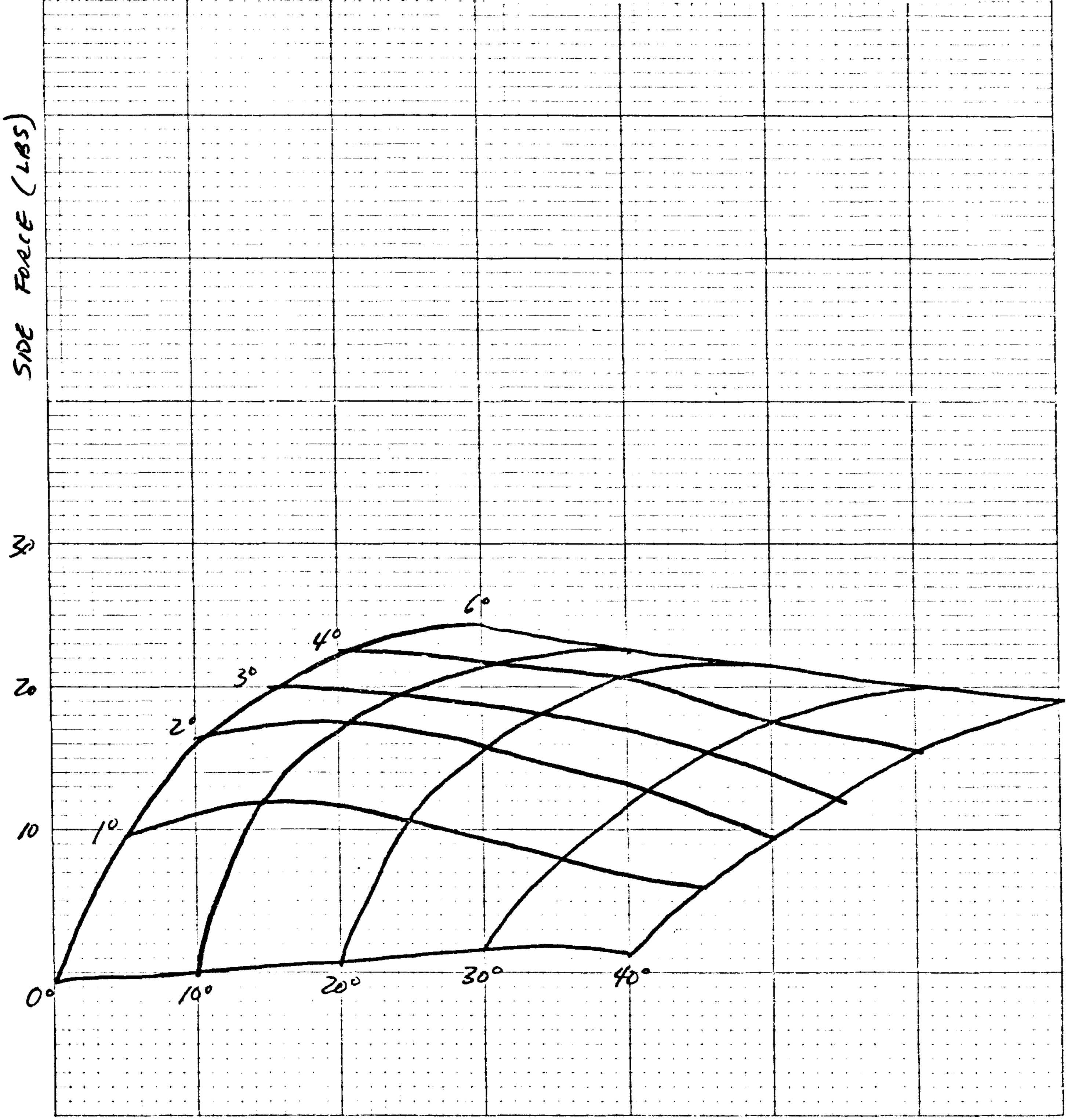

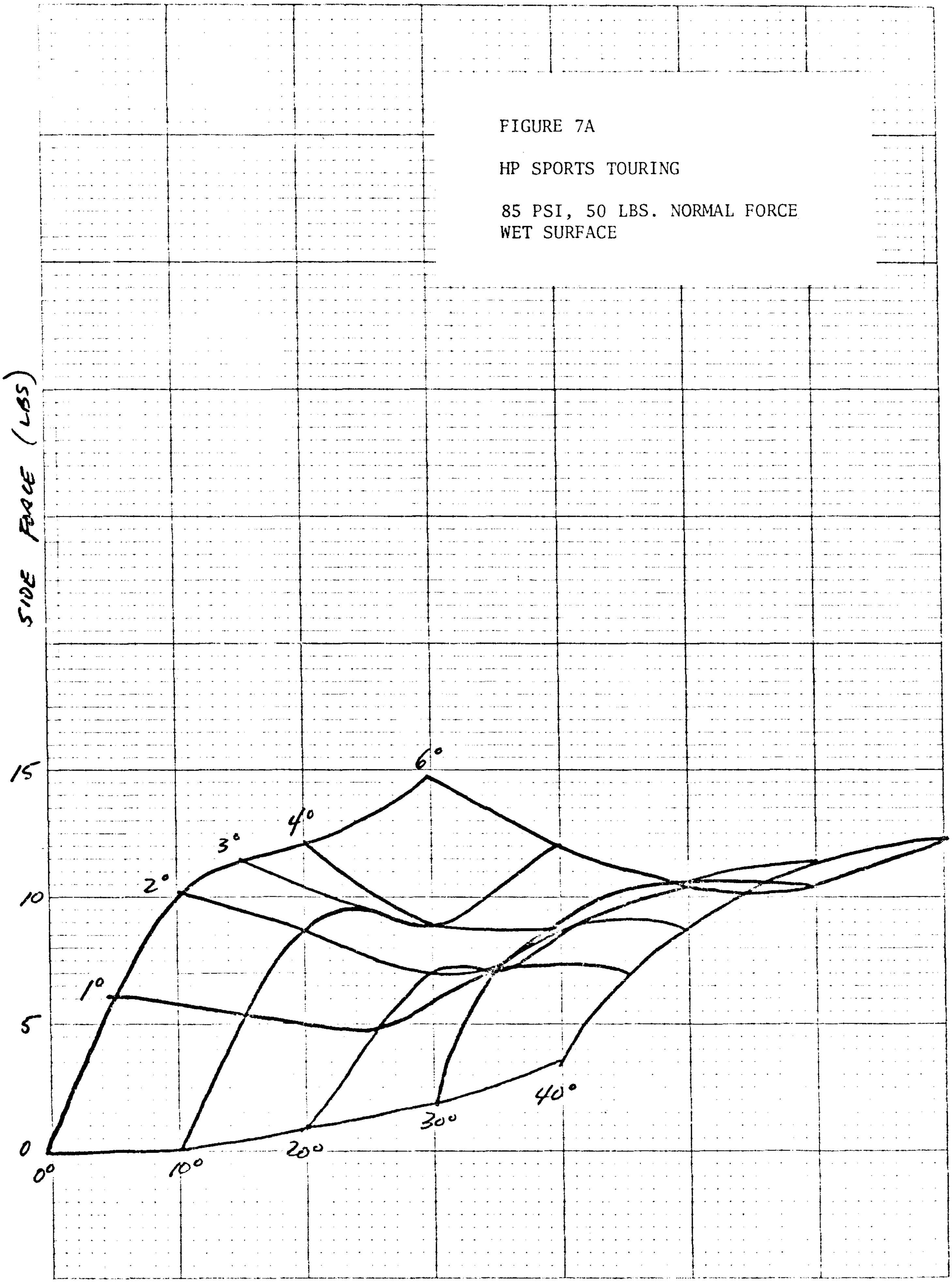

FIGURE 7A

HP SPORTS TOURING

85 PSI, 50 LBS. NORMAL FORCE
WET SURFACE

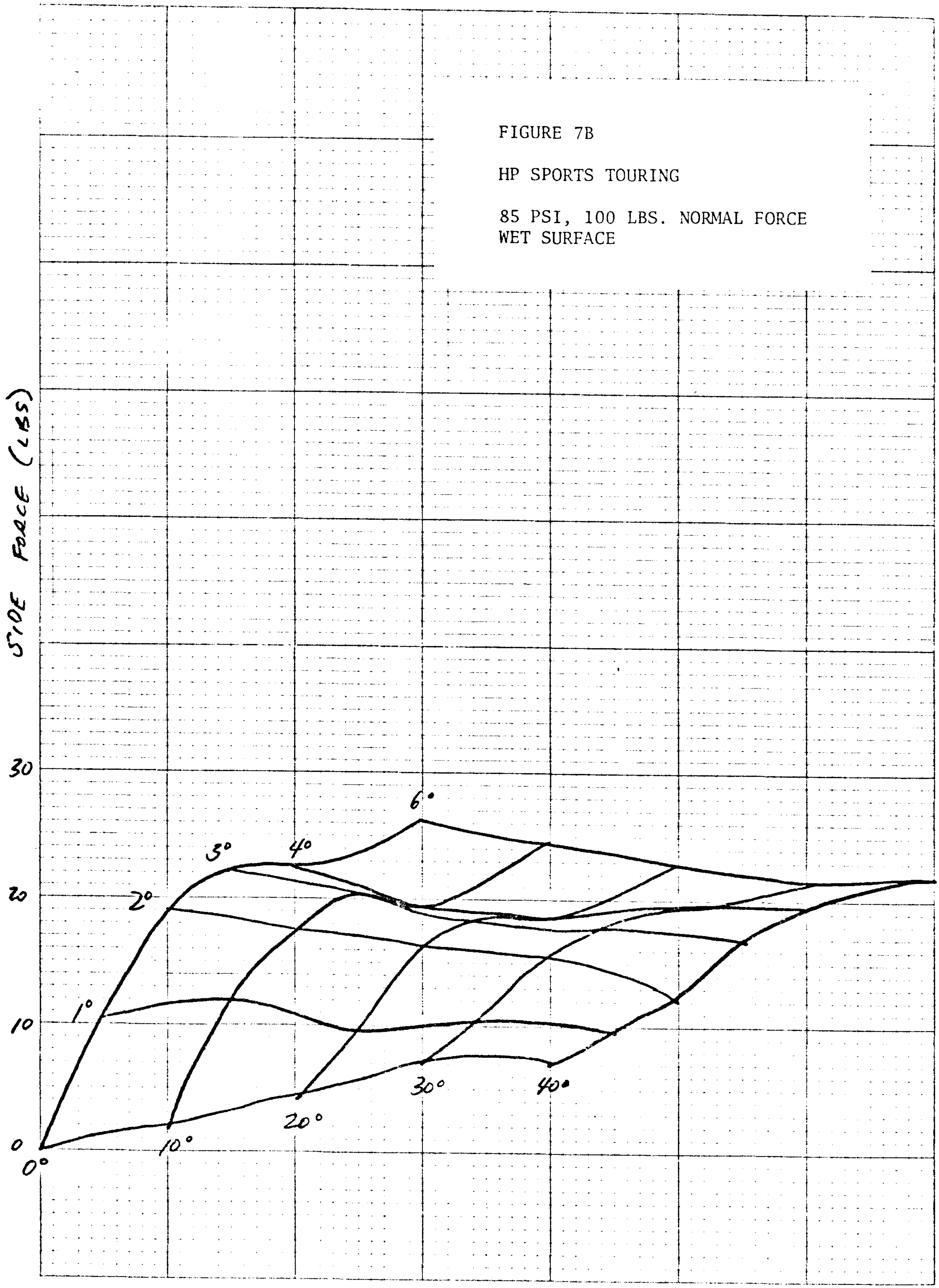
FIGURE 7B
HP SPORTS TOURING
85 PSI, 100 LBS. NORMAL FORCE
WET SURFACE
SIDE FORCE (LBS)
30
20
10
0
0°
1°
2°
3°
4°
6°
10°
20°
30°
40°

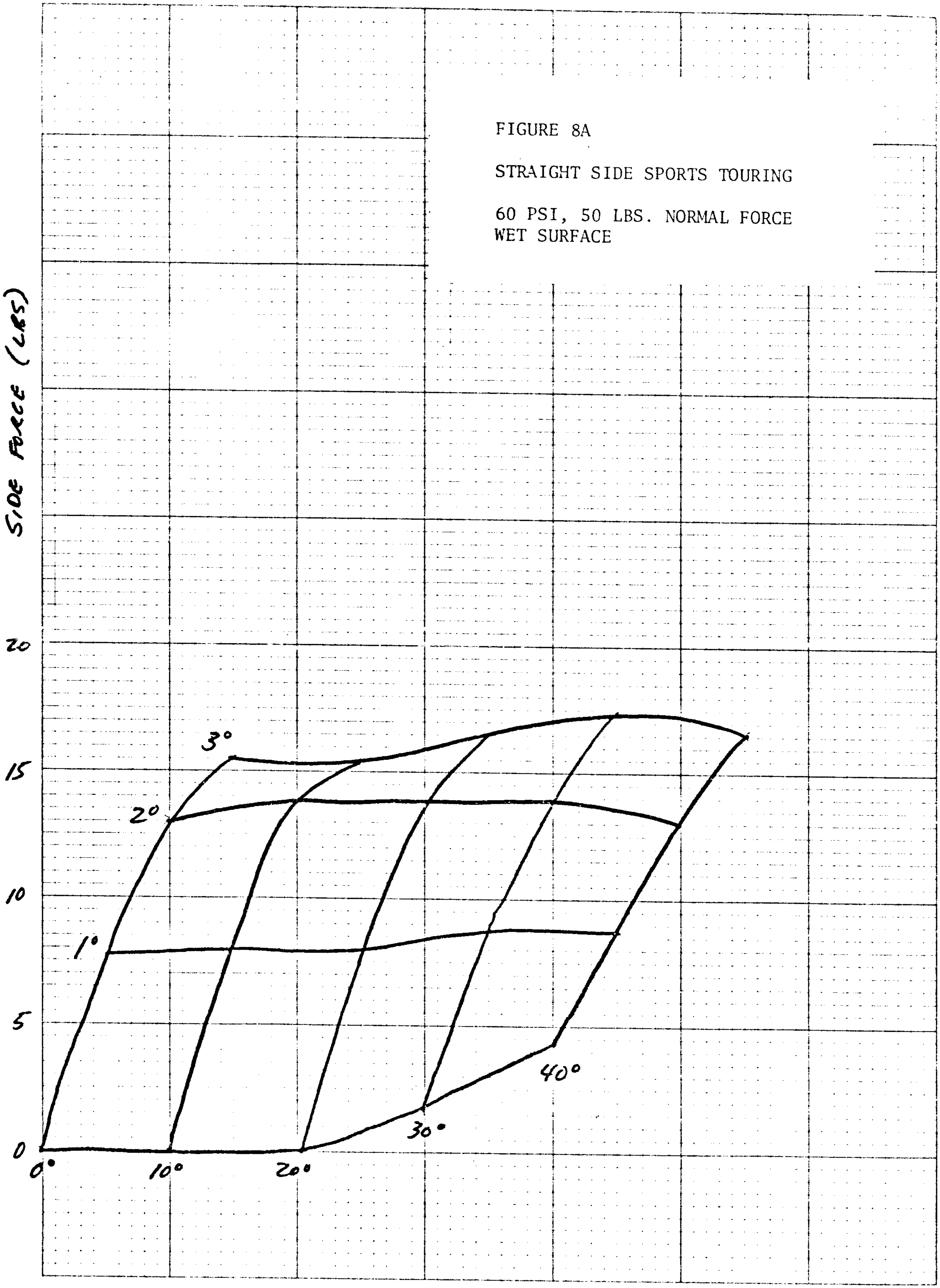

FIGURE 8A

STRAIGHT SIDE SPORTS TOURING

60 PSI, 50 LBS. NORMAL FORCE
WET SURFACE

FIGURE 8B

STRAIGHT SIDE SPORTS TOURING

60 PSI, 100 LBS. NORMAL FORCE
WET SURFACE